Tanzania Journal of Engineering and Technology 2024, **43**(4):54 - 65
OPEN ACCESS articles distributed under Creative Commons Attribution Licence [CC BY-ND]
Websites: https://ajol.org/tjet; https://tjet.udsm.ac.tz

ISSN 1821-536X (**print**); ISSN 2619-8789 (**electronic**)
https://doi.org/10.52339/tjet.v43i4.1036

Regular Research Manuscript

Efficient Operation of Direct Coupled Solar Home PV System: A Case of Solar Home PV System Installed in Dodoma, Tanzania

Sarah P. Ayeng'o

Department of Mechanical and Industrial Engineering, University of Dar es Salaam, P.O Box 35131, Dar es Salaam, Tanzania.
Corresponding author: ayengo@udsm.ac.tz

ABSTRACT

Direct coupled Photovoltaic (PV) system is a common topology among most of the off-grid communities in the world. This topology has less components hence resulting in low investment costs. However, it suffers much losses when battery operating voltage is far from maximum power point voltage of PV modules. This scenario can be attributed by different factors such as; variation in solar radiation, load profile and temperature. Efficient operation of these systems is required in order to reduce losses. Usually in direct coupled system, PV modules are connected in parallel with batteries through a charge controller hence making PV output to depend solely on battery operating points. For losses reduction, a proper voltage range of battery and PV modules has to be selected. The challenge to many technicians is on proper selection of ranges of voltages of battery and PV module. This results in installed PV systems being operating away from maximum power point hence much losses. This paper presents a model of solar home PV system developed using MATLAB software. Two types of solar PV modules; A Copper, Indium, Gallium, Selenium (CIGS) thin film and a polycrystalline PV module with 24V lithium nickel cobalt aluminum oxide as a storage were modeled. The Solar radiation data and load profiles were collected from Dodoma, Tanzania. In order to get optimum results, optimization tool was also developed by using genetic algorithm. For efficient operations of direct coupled PV systems, the ratio between 0.7 and 0.9 of battery to PV maximum power point voltages has been proposed. By using these ratios in PV system designing, one can have an assurance of operating PV system at minimum losses in areas with high solar radiation. This can be a simple method to be used when designing solar home system. However, more detailed analysis on battery capacity and PV modules are recommended.

ARTICLE INFO
Submitted: **July 26, 2024**
Revised: **Nov. 19, 2024**
Accepted: **Dec. 17, 2024**
Published: **Jan. 2025**

Keywords: *Maximum power point, off-grid system, direct coupled PV system, and battery energy storage.*

INTRODUCTION

In recent years, most of the off-grid communities in Tanzania have been sensitized and educated on the importance of using electricity for their day to day activities (Minja & Mushi, 2023). Electricity being an engine of development to any society, can be used for different purposes like lightning, powering appliances, food storage and cooking (Bertheau et al., 2014).

In general, electrification rate in Tanzania is still very low (Masenge & Mwasilu, 2020).

Only twelve years ago (Grimsby, Aune, & Johnsen, 2012) reported that, 86% of Tanzanian population was not connected to the national grid, of which most of them live in rural areas. (Bertheau *et. al.*, 2014) also reported that, electrification rate of the country is low of about 11 %, whereby in rural areas it falls to ranges below 2%. Two years later, another author (Moner-Girona *et. al*., 2016) reported also that, in Tanzania only about 14% of the population has access to electricity, with only 3% reaching rural areas.

There has been a remarkable increase in electricity access in recent years with data reports reaching up to 32.8 % of the whole Tanzanian population (Justo & Mushi, 2020). From this population, 65% of the electrified population is from urban areas and 18% of rural off-grid areas. Of the electrified population, 74.9% is electrified with national grid, 24.7% is electrified from solar PV systems and the remaining percentage (0.4%) is electrified from individual small diesel generators(Bastholm & Fiedler, 2018; Olukan & Emziane, 2014; Rocco, Fumagalli, Vigone, Miserocchi, & Colombo, 2021)). This has shown a significant improvement and increase of off-grid electrification in Tanzania especially with the use of solar PV systems.

The small percent of population using solar energy is expected to increase in the coming years due to the awareness which has been created on the use PV systems (Mruma & Ayeng'o, 2023). Not only that but also worldwide the cost of PV modules is decreasing (Kaombe & Katemi, 2023; Minja & Mushi, 2023). On the other hand, most of the off-grid population in Tanzania have no technical background on PV systems. Selection of correct PV module type, battery and size is still a challenge (Kasilima *et. al.*, 2024). Not only that but also large percent of the off-grid population lack knowledge on how to efficiently operate PV system. This leads to energy losses and early aging of some of the PV systems' components like batteries.

There are different types of PV panels which can be found in the market. They can be categorized depending on different technologies and they include first, second and third generation PV panels(Ibn-Mohammed *et. al.*, 2017; Ibrahim & Anani, 2017). First generation solar cells are also known as conventional cells. They are mostly made of silicon materials, include crystalline and amorphous cells and are the ones which are mostly available in the market (Vinod, Kumar, & Singh, 2018).

Second generation solar cells are thin film cells as for example cadmium telluride (CdTe), copper indium gallium diselenide (CIGS), and gallium arsenide (GaAs) cells. Third generation solar cells are mostly still in research phase. Furthermore, there is an emerging market of organic photovoltaic cells and perovskite (Ibn-Mohammed *et. al.*, 2017). Figure1 shows in brief the classification of PV modules.

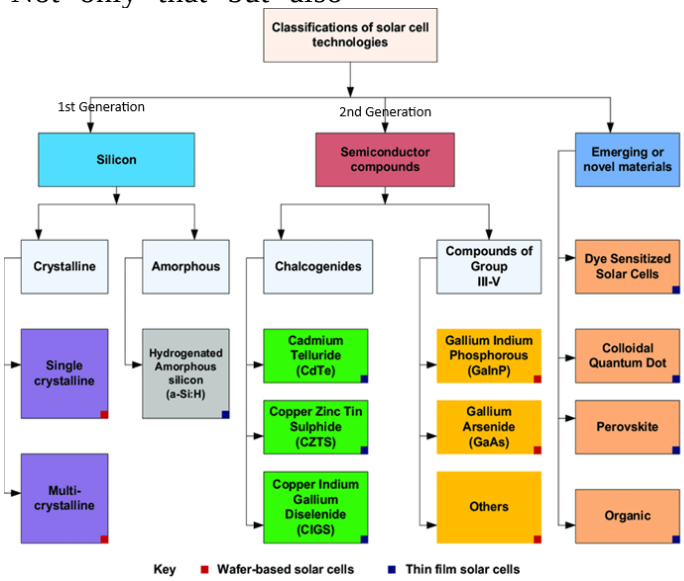

Figure 1: Classification of solar cell technologies (Ibn-Mohammed *et. al.*, 2017).

For solar PV systems, batteries are also of importance for electricity storage (Justo & Mushi, 2020). Although in the market there are different types of batteries, most of off-grid population uses lead-acid batteries (Kaombe & Katemi, 2023). This is due to the fact that lead-acid battery is a mature technology and its investment cost is lower compared to other technologies like lithium ion batteries(Hoppmann, Volland, Schmidt, & Hoffmann, 2014; Kwiecien, Schröer, Kuipers, & Sauer, 2017; Pavlov, 2017). (Paul Ayeng'o, Schirmer, Kairies, Axelsen, & Uwe Sauer, 2018) did a study by comparing cost of lead -acid and lithium-ion batteries for the lifetime of 20 years in the PV system. They found that solar home system (SHS) with Lithium Nickel Cobalt Aluminum Oxide (NCA) battery generally had a lower LCOE compared to the SHS with lead-acid battery. This was mainly due to both the longer life time of NCA batteries and the reduction of the price of NCA batteries as a result of significantly increasing global production scales.

Due to the fact that market have different types of PV module and batteries, proper ratio between battery and PV module voltage during PV system design has to be known, so as to easily select proper combination of battery and PV modules voltages of the designed system and have an assurance of operating the system efficiently. In this study, a directly coupled solar home PV model has been developed. 24V DC household using either Copper, Indium, Gallium, Selenium (CIGS) thin film or polycrystalline PV modules with lithium nickel cobalt aluminum oxide (NCA) has been studied.

By considering fluctuation of solar radiation, temperature and load profile, the developed model can select an optimal range of maximum power point voltage (U_{MPP}) of different PV modules. This is done by selecting the optimal number of PV cells connected in series. The ratio between battery nominal voltage and maximum power point voltage (U_{MPP}) can help easily selection of PV module and battery voltage in the market and have confidence that PV system will always be operated at high efficiency. The results presented in this paper, are from the study which was done in Dodoma, Tanzania however, the model can be adopted at any climatic area.

METHODS AND MATERIALS

Solar PV model

The developed PV model calculates first PV output at an inclined plane. MATLAB/Simulink programme was used in the development of the model. It then calculates current and voltage at maximum power point. The model uses solar radiation data (global, direct, diffuse and reflected radiation), temperature, PV module electrical data and inclination angle as input data (Ibrahim, El-Sebaii, Ramadan, & El-Broullesy, 2013; Justo & Mushi, 2020; Merei, Berger, & Sauer, 2013). Input solar radiation were measured at horizontal plane. Hence global solar radiation at an inclined plane was calculated as follows (Reddy, Reddy, & Kumar, 2017; Zaraket, Khalil, Aillerie, A. Vokas, & Salame, 2017).

$$H_t = H_b R_b + H_d R_d + (H_b + H_d) R_r \quad (1)$$

Where R_b, R_d and R_r are the ratios of beam (direct), diffuse and reflected solar radiation on the inlined plane to that on the horizontal plane, H_b and H_d are direct and diffuse radiation measured at horizontal plane, and H_t is the total solar radiation at the inclined plane.

Values of solar radiation at inclined plane are calculated using the following equations 2, 3 and 4. These represents the calculation for beam (direct), diffuse and reflected solar radiation at inclined plane respectively. Beam (direct) solar radiation at an inclined plane is calculated as,

$$H_b = H_{b,0}(cos(\theta) / \cos(\theta z)) \quad (2)$$

$H_{b,0}$ is the beam (direct) solar radiation measured at horizontal plane (W/ m²), θ and (θz) are the incidence angle of direct radiation on tilted surface and horizontal surface, respectively (°).

Diffuse solar radiation at an inclined plane is calculated as follows,

$$H_d = H_{d,0}(\frac{1}{2}(1 + cos(\beta))) \quad (3)$$

$H_{d,0}$ is the diffuse solar radiation measured at horizontal plane (W/ m²) and β is the inclination (tilt) angle (°). And reflected solar radiation at an inclined plane is also calculated as,

$$H_r = \alpha_s H_{t,0}(\frac{1}{2}(1 - cos(\beta))) \quad (4)$$

α_s is the ground reflectivity and $H_{t,0}$ is the global solar radiation at horizontal plane (W/ m²).

PV output current and voltage

The calculation of PV output for the direct-coupled PV system as a function of solar radiation H_t, temperature T, battery voltage U_{batt} and number of serial connected PV cells $N_{PV_{serial}}$ ($P(H_t, T, U_{batt}, N_{PV_{serial}})$) has been adopted from (Paul Ayeng'o, Axelsen, Haberschusz, & Sauer, 2019). Current at maximum power point is calculated as:

$$I_{MPP} = \frac{(\alpha_1 H_t)^2}{(\Gamma + (\alpha_1 H_t)} \quad (5)$$

H_t is the global solar radiation at inclined plane (W/ m²), α_1 and Γ are PV module constants (Paul Ayeng'o *et. al*., 2019). The voltage at maximum power point depends strongly on the PV module temperature and the solar radiation. The PV module temperature was calculated using the following equation (Vinod *et. al*., 2018; Traoré et al., 2018; (Mayanjo & Justo, 2023)).

$$T_{PV} = T_{amb} + (H_t \text{ x } T_{PVcoeff}) \quad (6)$$

T_{PV} is the PV module temperature (°C), T_{amb} is the ambient temperature (°C), H_t is the global solar radiation at inclined plane (W/ m²) and $T_{PVcoeff}$ is the coefficient temperature of the PV module set between 0.02 °C/W/m² for completely free standing panels with good heat dissipation and 0.04 °C/W/m² for poor cooling, directly mounted to the roof (Arbuzov *et. al*., 2015; Bellia *et. al*., 2014; Machniewicz *et. al.*, 2015; Merei *et. al*., 2013).

Now,

$$U_{MPP} = a_1 \, ln^2(H_t + 1) + \frac{a_2 \, ln(H_t+1) + a_3}{ln(H_t+1) + a_4} + C_t \, (T_{PV} - T_{ref}) \quad (7)$$

where U_{MPP} is the PV voltage at maximum power point (V), T_{ref} is the reference temperature (25 °C), C_t is the temperature coefficient describing the voltage decrease with the increase in temperature, a_1, a_2, a_3 and a_4 are parameters which are presented in detail by (Paul Ayeng'o *et. al*., 2019) . The theoretical power of a single PV module operated at maximum power point is then calculated in equation 8.

$$P_{MPP} = U_{MPP} \text{ x } I_{MPP} \quad (8)$$

$$P_{MPP} = N_s \text{ x } U_{MPP} \text{ x } N_p \text{ x } I_{MPP} \quad (9)$$

If several PV modules are connected in serial for the purpose of increasing output voltage and in parallel for increasing output current and power, equation 9 is applied. N_s is the number of PV modules in serial and N_p is the number of PV cells in parallel. Yearly energy generation when system is operated at maximum power point E_{mpp} and direct coupled topology $E_{dircoup}$ are calculated by integrating the generated powers (P_{mpp} and $P_{dircoup}$) which are power at maximum power points and when operated in a direct coupled topology respectively.

$$E_{mpp} = \int_0^t (P_{mpp}) dt \quad (10)$$

$$E_{dircoup} = \int_0^t (P_{dircoup}) dt \quad (11)$$

NCA battery model

The used battery model had nickel-cobalt-aluminum oxide at the positive electrode and graphite at negative electrode. The positive electrode cell material is more vulnerable for a thermal runaway (Chen e*t. al*., 2020). Figure 2 show the indication of different characteristic of NCA batteries either low, medium or high. It can be seen that, NCA batteries have high specific energy which makes it favourable for high energy applications. However, safety issues should be considered when using this type of battery especially at cell level to avoid thermal run away. Table 1 presents detailed values of different parameters of NCA batteries.

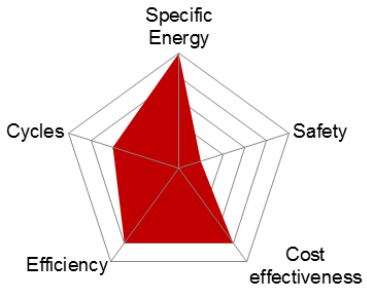

Figure 2: Characteristics of NCA batteries.

Table 1: NCA Battery Characteristics

System	NCA
Energy Density	80-220 Wh/kg 210-600 Wh/l
Power Density	1500-1900 W/kg 4000-5000 W/l
Operating temperature range (°C)	−20 to +60
Cycle Life	1500 - 5000
Calendar life	10-20 years
Battery cost	840,000 – 2,240,000 Tsh/kWh

NCA battery model was adopted from the model presented by (Magnor, Gerschler, Ecker, Merk, & Sauer, 2009); Chen *et. al*., 2020; (Schiffer *et. al*., 2007). Battery state of charge was calculated by using Coulomb counting equation as presented in equation 13.

$$SOC(t) = SOC_0 + \int_0^t (I_{eff}(t)/C_{act}(t)dt \quad (13)$$

$SOC(t)$ is the actual state of charge in percentage, SOC_0 is the initial state of charge in percentage, $I_{eff}(t)$ is the effective battery current that is used to charge or discharge the battery and $C_{act}(t)$ is the actual battery capacity in Ah.

Load profile

Most of rural households have low electrical energy consumption. In this study, household which consumes 0.3 kWh per day was used with its daily profile as presented in figure 3. It can be seen clearly from the graph that; this household uses more electricity at night when there is no solar radiation. For such household, the use of battery is essential.

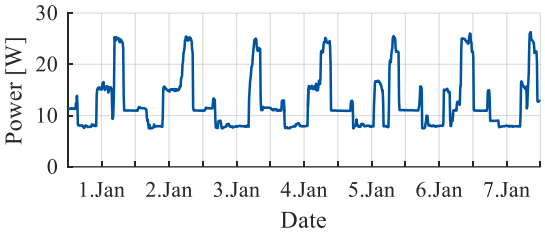

Figure 3: Household load profile.

Electrical data sheet of polycrystalline

In this study, polycrystalline and Copper, Indium, Gallium, Selenium (CIGS) thin film PV modules were used. The modules have 54 and 100 number of cells connected in series. They have 0.62V and 0.59V cell voltages. Table 2 describes the electrical data at standard test condition (STC is 25°C and 1000 W/m²). The I-V-P curve and the battery operating window for both types of PV

modules are presented in Figures 4 (a) and 4 (b) respectively.

Table 2: Electrical data sheet of polycrystalline and CIGS modules

Electrical data (at STC)	Polycrystalline	CIGS
Max. power (Pmax)	210 W	130 W
Max. power voltage (Umpp)	26.4 V	44.5 V
Max. power current (Impp)	7.95 A	2.92 A
Open circuit voltage (Uoc)	33.6 V	59.3 V
Short circuit current (Isc)	8.33 A	3.34 A

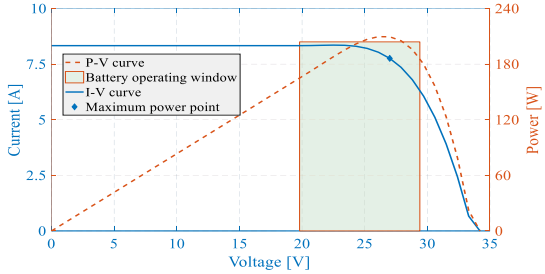

(a)

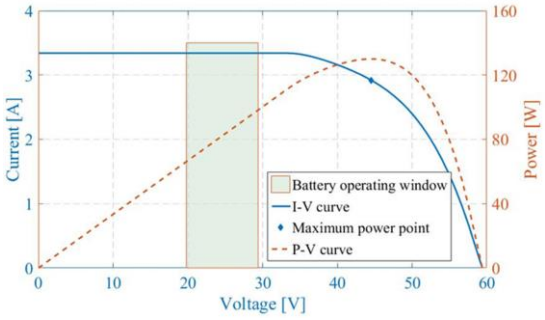

(b)

Figure 4: I-V-P curve for polycrystalline and CIGS.

Since the battery used has 24V, it can be seen from Figures 4(a) and 4(b) that, the PV modules used were able to charge battery to its full capacity. However, there is a challenge of operating PV module at low efficient region especially for the presented CIGS module. A proper selection of PV module and battery is required to avoid operating PV module at low efficient region method in this area. (Asprone, *et. al*., 2008).

System optimization

In this study, optimization was done by using a genetic algorithm (GA) (Figure 5) which was implemented in Matlab. The optimization runtime was around 3-4 hours by using a discrete step solver. Moreover, a simulation step of 600 seconds in real time was used which further reduced the computing effort. A parallelization of the GA was done which further shortened the run time, hence making the computation and the analysis of data more efficient.

The basic structure of the operation of a GA is as follows (Nyirenda, Kihedu, Kimambo, & Nielsen, 2024; Traoré, Elgothamy, & Zohdy, 2018):

i. A population is generated randomly (eg. population size of 200). This population consists of a number of individuals, which in turn consist of chromosomes.

ii. A fitness function is computed using the available chromosomes. The individuals with the best fitness value for the case of this study, the individuals with lowest levelized cost of energy (LCOE) pass to the next generation.

iii. Using genetic operators such as crossover and mutation, a new generation is created.

iv. The population with the chromosome set revealing the best fitness values and the newly created populations are computed for the next generation.

v. For obtaining final results, step 2 to 4 is repeated until a stop criterion is met. In this study, the number of generations was set to 150. The GA then selected the best chromosome set after finishing 150 iterations.

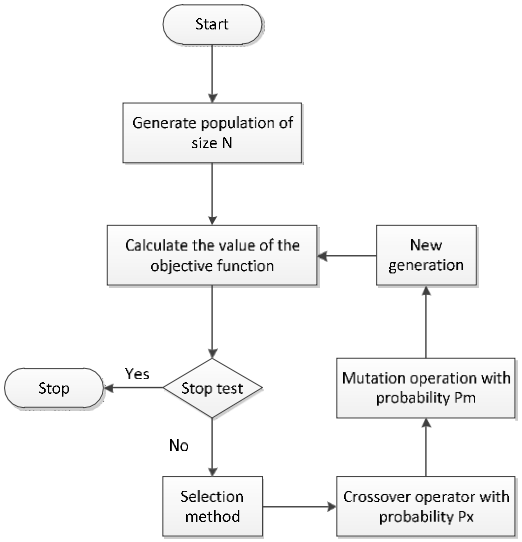

Figure 5: Genetic algorithm.

The levelized cost of energy (LCOE) was considered as a fitness function during optimization process (Kasilima, Ayeng'o, & Nshama, 2024). Low LCOE was preferred but this depended strongly on the equipment costs and the real energy supplied to cover the load. Fitness function was calculated as:

$$LCOE = \frac{A}{E_{real\_supplied}} \quad (12)$$

$$A = NPV \times (1+i)^{-n}/i \quad (13)$$

whereby A is the annuity, NPV is the total net present value, i is the interest rate and $E_{real\_supplied}$ is the real load which is covered by PV system. Tables 3 and 4 represent the optimized parameters and the costs used in the calculation of LCOE.

Table 3: Optimized parameters

Parameter	Unit	Increment	Lower boundary	Upper boundary
Inclination angle	°	1	0	90
Azimuth angle	°	1	90 (East)	270 (West)
SOC max	%	1	0	100
SOC min	%	1	0	100
Battery capacity	Wh	1	5	500
Number of PV cells in series	-	1	1	200
Number of PV cells in parallel	-	1	1	500

Table 4: Cost of system components

Component	Price
PV modules	1,200,000 Tsh/kWp
Charge controller	140,000 Tsh
NCA battery	1,120,000 Tsh/kWh
Interest rate (with inflation)	6.67%

RESULTS AND DISCUSSIONS

Optimal solar PV module

The original simulated Polycrystalline and CIGS modules have 54 and 100 cells connected in series respectively. After optimization process, the optimal number of PV cells connected in series was 61 and 65 respectively. More optimal results are as presented in table 5.

Table 5: Optimization results for Polycrystalline PV panels

Parameter	Unit	Polycrystalline	CIGS
Inclination angle	◦	7	5
Azimuth angle	◦	182	185
SOC maximum	%	83	86
SOC minimum	%	0	5
Number of PV cells in series	-	61	65
Number of PV cells in parallel	-	5	12
Peak power	Wp	118.6	101.4

From the optimal sizes of the simulated PV modules, a comparison was done between PV system which is directly coupled with the battery and PV system operated at maximum power point. It can be seen clearly from figure 6 (a) and (b) that, most of the time, direct coupled system was operated near the

maximum power point hence efficiently operated.

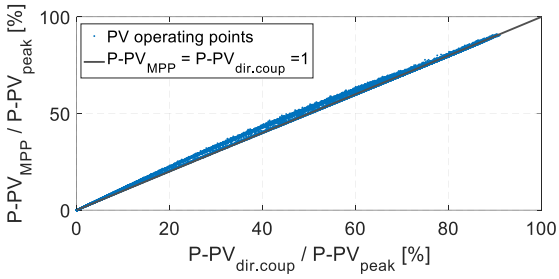

(a)

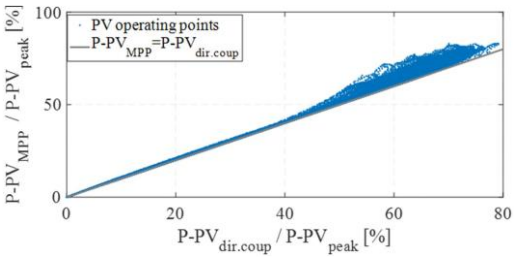

(b)

Figure 6: A comparison between PV system directly coupled to the battery and PV system operated at maximum power point for Polycrystalline and CIGS modules, respectively.

Optimal ratio of battery to maximum power point PV voltages

Analysis was done to find the optimal number of PV cells connected in series for both of the used PV modules. This optimal number allows direct coupled system to operate at low losses (high efficiency). The optimal number of PV cells connected in series lie between 53 and 65 for polycrystalline and 63 and 80 for CIGS instead of 53 and 100 cells of the original modelled PV modules. Figure 7(a) and (b) shows the percentage of losses which can be accounted with the change in the serial number of PV cells for polycrystalline and CIGS modules.

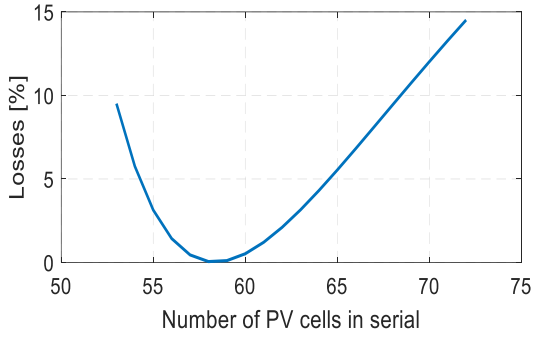

(a)

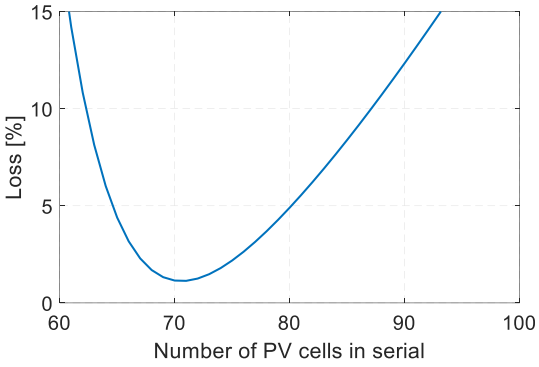

(b)

Figure 7: Optimal numbers of PV cells connected in series for Polycrystalline and CIGS, respectively.

Losses in this study is calculated as:

$$\left(\frac{E_{mpp} - E_{dircoup}}{E_{mpp}}\right) \mathbf{x\ 100\%} \qquad (14)$$

where as $E_{dircoup}$ is the direct-coupled PV system yearly generated energy and E_{mpp} is the yearly energy generated when the PV system is operated at its maximum power points.

From Figure 7 (a) and (b), it can be seen that, PV module with number of PV cells connected in series from 53 to 65; and 63 and 80 for polycrystalline and CIGS respectively can be operated at high efficiency when connected to 24V NCA battery. From the proposed range of optimal number of PV cells, the optimal battery to PV modules ratio is calculated as follows:

$$\text{Optimal ratio} = U_{bat\_nom} \,/\, U_{MPP} \qquad (15)$$

The proposed battery to PV module ratio is 0.7 to 0.9. Within this ratio, one can have an assurance when selecting the PV system, that the system will efficiently be operated. This

ratio can also be used by other types of PV modules and batteries during PV system design.

VALIDATION OF THE DEVELOPED PV MODEL

For the purpose of validating the proposed model, laboratory tests were done. The tests were done bychanging the number of cells in serial for polycrystalline PV module, load profiles and solar radiation. The following equipment were used: PV simulator, load simulator, battery and charge controller. Selecting the type of PV module and changing the number of cells were done by changing the STC (standard test condition) parameters of the optimized modules in the PV simulator. These included U_{oc}, I_{sc}, U_{MPP} and I_{MPP}.

In this section, the validation for using polycrystalline module is presented. Table 6 presents the STC parameters which were used as input to the PV simulator. In this test a bigger battery with 130 Ah was used because of the availability. The numberof optimized PV modules in parallel was increased to 30 by increasing I_{MPP} and I_{sc} so as to cover the given load. 54, 58 and 61 PV cells in serial were used.

The results from this test are presented in Figures 8 to 9. Starting with 54 cells, which was the original parameterized module, the presented figures show how the system operated very near to the U_{MPP}.

Table 6: New data sheet used for polycrystalline PV modules

No	No. cells in serial	U_{mpp}	I_{mpp}	U_{oc}	I_{sc}
1	54 (original)	26.522	23.61	33.60	24.99
2	58	28.4756	23.61	36.09	24.99
3	61	29.9485	23.61	37.96	24.99

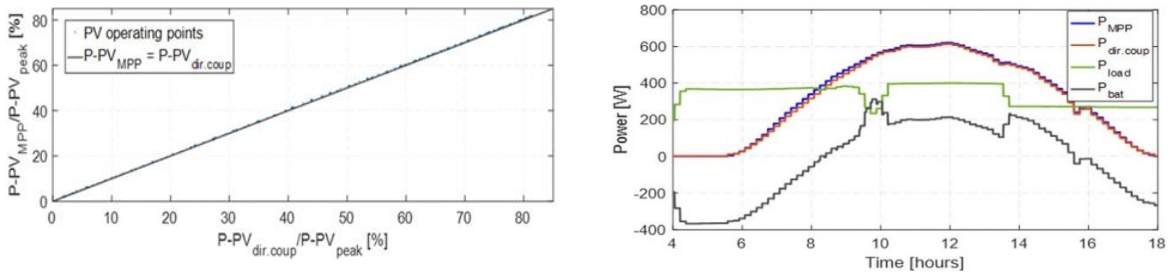

(a) (b)

Figure 8: Power output at MPP and directly coupled system with 54 cells.

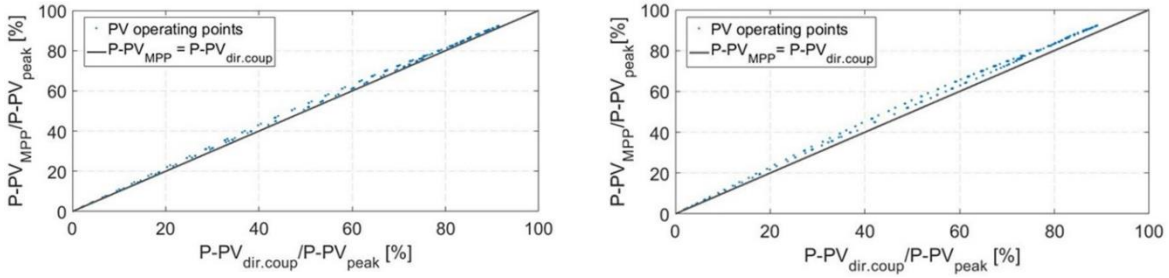

(a) (b)

Figure 9: Power output at directly coupled system and at MPP with a) 58 cells and b) 61 cells.

Sigalotti, Klapp, & Gesteira, (2021) carried

Table 7 shows the efficiencies reached during

laboratory tests. High efficiencies could be reached when a system was connected at a direct-coupled topology. Low solar radiation of 200 W/m^2 and high solar radiation of 1000 W/m^2 were used.

Table 7: System efficiency with different serial connected PV cells

Item	Number of cells	Efficiency (%)
High solar radiation	54	97.4
	58	99
	61	94.4
Low solar radiation	58	95

CONCLUSION AND RECOMMENDATIONS

In this study, a simple method of selecting battery and PV module voltage has been presented. A ratio of nominal battery voltage to maximum power point voltage of PV modules have been proposed. The ratio is between 0.7 to 0.9. This can help in the selection of the best combination of PV and battery voltages for the direct coupled system and at the same time having a confidence of efficiently operating PV system. However, the sizing of battery capacity and PV maximum power should also be done. The proposed methodology can be adapted at any region using different PV modules, batteries and electrical load sizes.

NOMENCLATURE

CdTe	Cadmium telluride
CIGS	Copper indium gallium diselenide
GA	Genetic algorithm
GaAs	Gallium arsenide
LCOE	Levelized cost of energy
MPP	Maximum power point
NCA	Nickel cobalt aluminum oxide battery
PV	Photovoltaic
SHS	Solar home system
STC	Standard Test Condition

REFERENCES

Arbuzov, Y. D., Evdokimov, V. M., Majorov, V. A., Saginov, L. D., & Shepovalova, O. V. (2015). Silicon PV Cell Design and Solar Intensity Radiation Optimization for CPV Systems. *Energy Procedia,* **74**, 1543–1550. doi:10.1016/j.egypro.2015.07.717

Bastholm, C., & Fiedler, F. (2018). Techno-economic study of the impact of blackouts on the viability of connecting an off-grid PV-diesel hybrid system in Tanzania to the national power grid. *Energy Conversion and Management*, **171**, 647–658. doi:10.1016/j.enconman.2018.05.107

Bellia, H., Youcef, R., & Fatima, M. (2014). A detailed modeling of photovoltaic module using MATLAB. *National Research Institute of Astronomy and Geophysics Journal of Astronomy and Geophysics*, **3**(1), 53–61. doi:10.1016/j.nrjag.2014.04.001

Bertheau, P., Cader, C., Müller, H., Blechinger, P., Seguin, R., & Breyer, C. (2014). Energy Storage Potential for Solar Based Hybridization of Off-grid Diesel Power Plants in Tanzania. *Energy Procedia*, **46**, 287–293. doi:10.1016/j.egypro.2014.01.184

Chen, T., Jin, Y., Lv, H., Yang, A., Liu, M., Chen, B., et al. (2020). Applications of Lithium-Ion Batteries in Grid-Scale Energy Storage Systems. *Transactions of Tianjin University*, **26**(3), 208–217. doi:10.1007/s12209-020-00236-w

Grimsby, L. K., Aune, J. B., & Johnsen, F. H. (2012). Human energy requirements in Jatropha oil production for rural electrification in Tanzania. *Energy for Sustainable Development*, **16**(3), 297–302. doi:10.1016/j.esd.2012.04.002

Hoppmann, J., Volland, J., Schmidt, T. S., & Hoffmann, V. H. (2014). The economic viability of battery storage for residential solar photovoltaic systems – A review and a simulation model. *Renewable and Sustainable Energy Reviews*, **39,** 1101–1118. doi:10.1016/j.rser.2014.07.068

Ibn-Mohammed, T., Koh, S., Reaney, I. M.,

Acquaye, A., Schileo, G., Mustapha, K. B., & Greenough, R. (2017). Perovskite solar cells: An integrated hybrid lifecycle assessment and review in comparison with other photovoltaic technologies. *Renewable and Sustainable Energy Reviews*, **80**, 1321–1344. doi:10.1016/j.rser.2017.05.095

Ibrahim, A., El-Sebaii, A. A., Ramadan, M. R. I., & El-Broullesy, S. M. (2011). Estimation of solar irradiance on tilted surfaces facing south for Tanta, Egypt. *International Journal of Sustainable Energy*, **32**(2), 111–120. doi:10.1080/14786451.2011.601814.

Ibrahim, H., & Anani, N. (2017). Variations of PV module parameters with irradiance and temperature. *Energy Procedia*, **134**, 276–285. doi:10.1016/j.egypro.2017.09.617

Justo, J. J., & Mushi, A. T. (2020). Performance Analysis of Renewable Energy Resources in Rural Areas: A Case Study of Solar Energy. *Tanzania Journal of Engineering and Technology*, **39**(1), 1–12. doi:10.52339/tjet.v39i1.514

Kaombe, D., & Katemi, R. J. (2023). Lead Acid Battery Recycling in the Current Tanzania Industrialization Drive: Challenges and Opportunities. *Tanzania Journal of Engineering and Technology*, **41**(4), 106–118. doi:10.52339/tjet.v41i4.794

Kasilima, J., Ayeng'o, S., & Nshama, E. (2024). An Optimization Tool for a Standalone Photovoltaic System. *Tanzania Journal of Engineering and Technology*, **43**(1), 87–101. doi:10.52339/tjet.v43i1.968

Kwiecien, M., Schröer, P., Kuipers, M., & Sauer, D. U. (2017). Current research topics for lead–acid batteries. *4- Lead-Acid Batteries for Future Automobiles* (pp. 133–146). Elsevier. doi:10.1016/B978-0-444-63700-0.00004-

Machniewicz, A., Knera, D., & Heim, D. (2015). Effect of Transition Temperature on Efficiency of PV/PCM Panels. *Energy Procedia*, **78**, 1684–1689. doi:10.1016/j.egypro.2015.11.25

Magnor, D., Gerschler, J. B., Ecker, M., Merk, P., & Sauer, D. U. (2009). Concept of a Battery Aging Model for Lithium-Ion Batteries Considering the Lifetime Dependency on the Operation Strategy. 24th European Photovoltaic Solar Energy Conference doi: 10.4229/24thEUPVSEC2009-4BO.11.3

Masenge, I. H., & Mwasilu, F. (2020). Modeling and Control of Solar PV with Battery Energy Storage for Rural Electrification. *Tanzania Journal of Engineering and Technology*, **39**(1), 47–58. doi:10.52339/tjet.v39i1.518

Mayanjo, S., & Justo, J. (2023). Development of Solar PV Systems for Mini-Grid Applications in Tanzania. *Tanzania Journal of Engineering and Technology*, **42**(1), 200–212. doi:10.52339/tjet.v42i1.899

Merei, G., Berger, C., & Sauer, D. U. (2013). Optimization of an off-grid hybrid PV–Wind–Diesel system with different battery technologies using genetic algorithm. *Solar Energy*, **97**, 460–473. doi:10.1016/j.solener.2013.08.016

Minja, M., & Mushi, A. (2023). Design of International Airport Hybrid Renewable Energy System. *Tanzania Journal of Engineering and Technology*, **42**(1), 46–57. doi:10.52339/tjet.v42i1.887

Moner-Girona, M., Ghanadan, R., Solano-Peralta, M., Kougias, I., Bódis, K., Huld, T., & Szabó, S. (2016). Adaptation of Feed-in Tariff for remote mini-grids: Tanzania as an illustrative case. *Renewable and Sustainable Energy Reviews*, **53**, 306–318. doi:10.1016/j.rser.2015.08.055

Mruma, I. S., & Ayeng'o, S. P. (2023). Designing a Model of Solar Photovoltaic Water Pumping System for Off-Grid Localities in Tanzania. *Tanzania Journal of Engineering and Technology*, **42**(3), 154–170. doi:10.52339/tjet.v42i3.963

Nyirenda, E., Kihedu, J., Kimambo, C., & Nielsen, T. (2024). Optimization Pump as Turbine Coupled to a Self-Excited Induction Generator Using Multi-Objective Genetic Algorithm. *Tanzania Journal of Engineering and Technology*, **43**(1), 133–143.

doi:10.52339/tjet.v43i1.983

Olukan, T. A., & Emziane, M. (2014). A Comparative Analysis of PV Module Temperature Models. *Energy Procedia*, **62**, 694–703. doi:10.1016/j.egypro.2014.12.433

Paul Ayeng'o, S., Axelsen, H., Haberschusz, D., & Sauer, D. U. (2019). A model for direct-coupled PV systems with batteries depending on solar radiation, temperature and number of serial connected PV cells. *Solar Energy*, **183**, 120–131. doi:10.1016/j.solener.2019.03.010

Paul Ayeng'o, S., Schirmer, T., Kairies, K.-P., Axelsen, H., & Uwe Sauer, D. (2018). Comparison of off-grid power supply systems using lead-acid and lithium-ion batteries. *Solar Energy*, **162**, 140–152. doi:10.1016/j.solener.2017.12.049

Pavlov, D. (2017). Invention and Development of the Lead–Acid Battery. Chapter in a Book: *Lead-Acid Batteries: Science and Technology* (pp. 3–32). Elsevier. doi:10.1016/B978-0-444-52882-7.10001-1

Reddy, G. S., Reddy, T. B., & Kumar, M. V. (2017). A MATLAB based PV Module Models analysis under Conditions of Nonuniform Irradiance. *Energy Procedia*, **117**, 974–983. doi:10.1016/j.egypro.2017.05.218

Rocco, M. V., Fumagalli, E., Vigone, C., Miserocchi, A., & Colombo, E. (2021). Enhancing energy models with geo-spatial data for the analysis of future electrification pathways: The case of Tanzania. *Energy Strategy Reviews*, **34**, 100614. doi:10.1016/j.esr.2020.100614

Schiffer, J., Sauer, D. U., Bindner, H., Cronin, T., Lundsager, P., & Kaiser, R. (2007). Model prediction for ranking lead-acid batteries according to expected lifetime in renewable energy systems and autonomous power-supply systems. *Journal of Power Sources*, **168**(1), 66–78. doi:10.1016/j.jpowsour.2006.11.092

Traoré, A., Elgothamy, H., & Zohdy, M. A. (2018). Optimal Sizing of Solar/Wind Hybrid Off-Grid Microgrids Using an Enhanced Genetic Algorithm. *Journal of Power and Energy Engineering*, **6**(5), 64–77. doi:10.4236/jpee.2018.65004

Vinod, Kumar, R., & Singh, S. K. (2018). Solar photovoltaic modeling and simulation: As a renewable energy solution. *Energy Reports*, **4**, 701–712. doi:10.1016/j.egyr.2018.09.008

Zaraket, J., Khalil, T., Aillerie, M., A. Vokas, G., & Salame, C. (2017). The Effect of Electrical stress under temperature in the characteristics of PV Solar Modules. *Energy Procedia*, **119**, 579–601. doi:10.1016/j.egypro.2017.07.083